Biochimica et Biophysica Acta 1837 (2014) 792–801

Contents lists available at ScienceDirect

Biochimica et Biophysica Acta

journal homepage: www.elsevier.com/locate/bbabio

NADPH fluorescence in the cyanobacterium *Synechocystis* sp. PCC 6803: A versatile probe for *in vivo* measurements of rates, yields and pools

Jocelyn Kauny, Pierre Sétif *

iBiTec-S, CNRS UMR 8221, CEA Saclay, 91191 Gif-sur-Yvette, France

ARTICLE INFO

Article history:
Received 19 September 2013
Received in revised form 10 January 2014
Accepted 13 January 2014
Available online 24 January 2014

Keywords:
Ferredoxin–NADP$^+$-oxidoreductase
Calvin–Benson cycle
Cyanobacteria
NADP pool
Ferredoxin
FNR bottleneck

ABSTRACT

We measured the kinetics of light-induced NADPH formation and subsequent dark consumption by monitoring *in vivo* its fluorescence in the cyanobacterium *Synechocystis* PCC 6803. Spectral data allowed the signal changes to be attributed to NAD(P)H and signal linearity *vs* the chlorophyll concentration was shown to be recoverable after appropriate correction. Parameters associated to reduction of NADP$^+$ to NADPH by ferredoxin–NADP$^+$-oxidoreductase were determined: After single excitation of photosystem I, half of the signal rise is observed in 8 ms; Evidence for a kinetic limitation which is attributed to an enzyme bottleneck is provided; After two closely separated saturating flashes eliciting two photosystem I turnovers in less than 2 ms, more than 50% of the cytoplasmic photoreductants (reduced ferredoxin and photosystem I acceptors) are diverted from NADPH formation by competing processes. Signal quantitation in absolute NADPH concentrations was performed by adding exogenous NADPH to the cell suspensions and by estimating the enhancement factor of *in vivo* fluorescence (between 2 and 4). The size of the visible (light-dependent) NADP (NADP$^+$ + NADPH) pool was measured to be between 1.4 and 4 times the photosystem I concentration. A quantitative discrepancy is found between net oxygen evolution and NADPH consumption by the light-activated Calvin–Benson cycle. The present study shows that NADPH fluorescence is an efficient probe for studying *in vivo* the energetic metabolism of cyanobacteria which can be used for assessing multiple phenomena occurring over different time scales.

1. Introduction

NADPH is a key redox metabolite used in anabolic processes. In photosynthetic organisms under light conditions, it is produced from NADP$^+$ and reduced ferredoxin (Fd^1_{red}) by the enzyme ferredoxin–NADP$^+$-oxidoreductase (FNR) according to the reaction: 2 Fd_{red} + NADP$^+$ + H^+ → 2Fd_{ox} + NADPH, Fd_{ox} being oxidized ferredoxin. It is also produced in darkness by the oxidative pentose phosphate pathway. In cyanobacteria as in all oxygen-evolving photosynthetic organisms, CO_2 assimilation occurs *via* the Calvin–Benson cycle which depends upon ATP and NADPH formed during the light phase of photosynthesis. The FNR catalytic mechanism has been thoroughly investigated *in vitro* since more than 40 years and is known in great detail [1,2]. This contrasts to the *in vivo* context where there are still many uncertainties, both in chloroplasts and in cyanobacteria, concerning *e.g.* the role of the different FNR isoforms including their involvement in different electron transfer pathways [3,4] and the FNR localization and compartmentation [5–7]. Among the two isoforms of different sizes that can be encoded by the unique FNR gene of *Synechocystis* sp PCC 6803 (hereafter named *Synechocystis*) [3], the large isoform, which constitutes the most part of FNR under the presently-used photoautotrophic conditions, is bound to the phycobilisome (PBS) *via* its N-terminal domain [8] and is thought of being primarily involved in linear electron transfer [3].

Since a few years, a commercial spectrophotometer (DUAL-PAM, Walz, Effeltrich, Germany) is available which allows NADPH to be measured *in vivo* [9]. Pioneering studies were made in this area showing that NADPH fluorescence could be used for investigations in cyanobacteria [10] and later on in chloroplasts and leaves [11]. Different lifetimes of NADPH fluorescence were more recently detected in chloroplasts, and this observation has been associated to the occurrence of different forms of NADPH, either free or bound to proteins [12]. These authors nevertheless concluded for the possibility of a "continuous monitoring of light-induced changes of NADP redox state in chloroplasts", a sentence that our present work will support to some extent for cyanobacteria. In a recent technical note, Schreiber and Klughammer [9] reported an extensive, although preliminary, study of light-induced NADPH measurements in cyanobacteria, green algae and isolated chloroplasts. This last report was instrumental to our study, where a detailed study of NADPH light-induced formation

Abbreviations: Fd_{red}, reduced ferredoxin; Fd_{ox}, oxidized ferredoxin; FNR, ferredoxin–NADP$^+$-oxidoreductase; PM, photomultiplier; MF, measuring frequency; chl, chlorophyll; $(Fd\text{-}PSI\ acc.)_{red}$, reduced ferredoxin or PSI terminal acceptors; ρ_{NADPH}, yield of NADPH formation from $(Fd\text{-}PSI\ acc.)_{red}$; FEF, fluorescence enhancement factor; PBS, phycobilisomes; PSI, photosystem I; PSII, photosystem II

* Corresponding author. Tel.: +33 169089867.
E-mail addresses: jocelyn.kauny@gmail.com (J. Kauny), pierre.setif@cea.fr (P. Sétif).

0005-2728/$ – see front matter © 2014 Elsevier B.V. All rights reserved.
http://dx.doi.org/10.1016/j.bbabio.2014.01.009

and after-light decay was performed with the same spectrophotometer on cell suspensions of the cyanobacterium *Synechocystis*. Spectral data, light-induced kinetics and calibration procedures will be described which show that a considerable amount of information can be drawn from such data regarding, among other things, the rate and efficiency of NADPH formation after one or two flashes, the rate limitation during linear transfer, the pool quantitation and the time range of Calvin–Benson cycle activation.

2. Material and methods

2.1. Culture conditions and preparation

Wild type cells of *Synechocystis* were grown photoautotrophically in an illuminated incubator at 32 °C in a CO_2-enriched atmosphere and under continuous light of moderate intensity (50 μmol photons m^{-2} s^{-1}) up to a maximum concentration of 12 μg chl./ml. The medium composition, including 10 mM sodium bicarbonate, is described in [13]. As previously reported [9], a strong background fluorescence signal due to a fluorescent substance is secreted by the cyanobacteria during growth. For decreasing the level of background fluorescence, the cells were centrifuged at 4000 *g* for 5 min just before the measurements and resuspended in fresh growth medium. For every sample, the absorption spectrum of the cell suspension was measured with an Olis-modernized Aminco DW2 spectrophotometer where the contribution of light scattering is minimum. The chl. main absorption band in the red region was highly reproducible for all cultures grown from 3 to 12 μg chl./ml with a maximum at 679 nm and a peak ratio PBS to chl. (625 nm/679 nm) comprised between 0.94 and 1.06. From these data, we concluded that the IsiA protein was not present so that the chl. content of the cells arises only from core photosystem I (PSI) and photosystem II (PSII).

2.2. NADPH measurements

Light-induced measurements were performed at 32 °C using the NADPH/9-AA module [9] of a DUAL-PAM (Walz, Effeltrich, Germany) in a square 1 × 1 cm opened cuvette with WT cell suspensions. Fluorescence is excited at 365 nm by a LED and is detected by a photomultiplier (PM) between 420 and 580 nm, this wavelength region being selected with a broad-band colored filter. The cells were incubated for 6–10 min at 32 °C in darkness inside the spectrometer before data acquisition begun. When possible, the cell suspension was stirred between measurements with stirring being stopped 30 s before data acquisition (noise was larger with stirring). When the delay between two consecutive acquisitions during averaging was too short for stirring, data acquisition was stopped from time to time and the suspension was stirred during a short period (typically 1 min every 30 min). The absence of stirring for as long as 1 h had no visible effect on the signals.

The DUAL-PAM conditions were as follows. For all measurements except laser excitation, the standard geometric configuration was that shown in Fig. 1 in [9], except there was no DUAL-PD unit ("PD" for photodiode). When using laser excitation, the 10 × 10 × 50 mm quartz rod collecting the laser light was mounted opposite to the emitter unit DUAL-ENADPH ("E" in "ENADPH" is for emitter; The DUAL-ENADPH unit provides the measuring light for NADPH excitation and red actinic light as well) so that the DUAL-DR unit ("DR" for detector; the DUAL-DR unit is not used for detection in our measurements as detection is made with the photomultiplier but is nevertheless kept in the set-up as it provides red actinic light together with DUAL-ENADPH; in this way, the cell suspension is illuminated with actinic light from both opposite sides in the standard configuration) had to be mounted opposite to the PM. As DUAL-DR contributes to actinic excitation, this led to PM saturation with signal loss for *c.* 5 ms following 10 μs flashes (see Fig. 5A). It was checked that, in this last configuration (actinic light provided by ENADPH and DR at right angles), the signal elicited by 10 μs flashes is similar to that found when DUAL-DR is opposite to DUAL-EDNADH (standard configuration) despite the fact that excitation is less homogeneously distributed. For all measurements, the measuring light intensity (365 nm) was set at 4 (on a scale of 1 to 20 in the DUAL-PAM software) and the measuring frequency (MF) was set at 100 Hz in darkness. This ensured no detectable actinic effect of the measuring light. The time-averaged light intensity at a setting of 4 and at a MF of 100 Hz corresponds to 1.2×10^{-4} μmol photons m^{-2} s^{-1} (personal communication, Dr. Erhard Pfündel, Walz). The intensity is proportional to the setting (1 to 20) and to the MF. Under continuous illumination, MF was increased to 5000 Hz, thus decreasing the noise level whereas its actinic effect is negligible *vs.* that of the red actinic light, and set back to 100 Hz at the end of the illumination period. During flash measurements (10 μs flashes provided by the DUAL-PAM or laser flashes), MF was increased to 5000 Hz from 10 ms before the flash to 100 ms after the flash (or first flash in double flash measurements). This led to a significant actinic effect which had to be subtracted. The actinic red light (continuous light and 10 μs flashes) was provided by the DUAL-PAM: maximum intensity at 628 nm, 50% intensity at 620 and 635 nm. The intensities mentioned in the figures are those given by the DUAL-PAM software. For calibrating the signal level, exogenous NADPH was added to the cell suspension at a final concentration of 2 to 4 μM at the end of the measurements. The concentration of the stock NADPH solution was controlled by absorption ($\varepsilon = 6220$ M^{-1} cm^{-1} at 340 nm [14]). As the signal(s) induced by the first illumination period(s) was (were) slightly different from the following ones, preillumination cycles were used in most experiments, as detailed in each figure legend. The laser excitation (wavelength, 700 nm; duration, 6 ns; energy, 28 mJ) was provided by a dye laser (Sirah Laser- & Plasmatechnik) pumped by a frequency-doubled Nd:YAG laser (Quanta Ray, Spectra Physics). Digital averaging was used for all continuous light measurements (averaging 10 points) except those of Fig. 6 whereas no digital averaging was used for flash measurements.

When extensive averaging was used (Figs. 1–6) and/or when different signals had to be compared, several precautions were taken. We will first describe the case of measurements made without interference filter (excluding Figs. 1B/C and 2B/C). For continuous illumination experiments, the measurements following preillumination treatments were checked to be similar before averaging (one by one or by averages of 4 when the signal to noise ratio was not good enough). Then the average of these initial signals was checked to be similar to partial averages made during the course of the measurements. For flash experiments, averaging 100 measurements was necessary before any comparison was possible with a sufficient signal to noise ratio. Series of 100–200 averages were then compared, and found to be similar, before these series were themselves averaged. For the data of Fig. 5, single flash measurements were alternated with double flash measurements (in series of 100–200). For the data of Fig. 6, the signals were averaged by series of 20 measurements before the light intensity was changed. For a given intensity, 3 such series giving identical signals were themselves averaged.

When measuring spectra (Figs. 1B/C and 2B/C), it was not possible to check that there was no signal variability because of insufficient signal to noise ratio. Measurements with interference filters were alternated with measurements without interference filter and it was checked that these last measurements gave similar signals during the whole acquisition period. Moreover, for the experiments of Figs. 1 and 2, several samples were used (8 and 10, respectively) and the whole spectrum was measured for each sample.

A control experiment was made in order to check whether local pH changes could be involved in the slow kinetics of NAD(P)H fluorescence (Fig. 2A): It was checked, by measuring NADPH fluorescence in a standard commercial spectrofluorimeter (Cary Eclipse, Agilent Technologies) that the NADPH fluorescence spectrum and intensity are pH-independent in the pH range 7–10. We also checked that

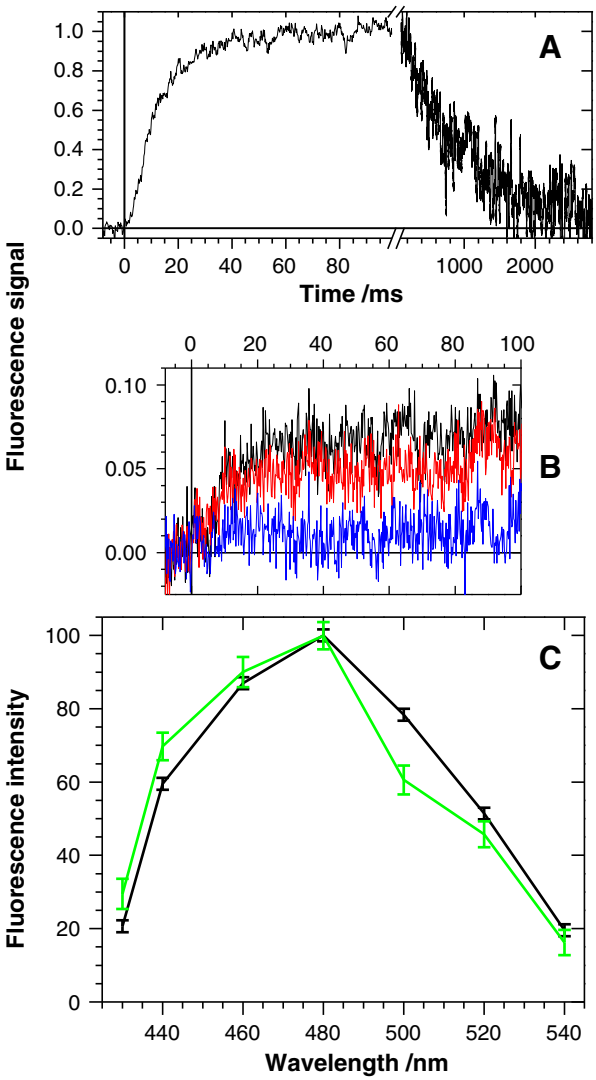

Fig. 1. Fluorescence kinetics induced by 10 μs flashes. Wavelengths were selected by using interference filters (FWHM ≈ 10 nm). One flash every 4 s. Cell suspension at a concentration of 2.5 μg chl./ml. *In vivo* measurements between −400 and 2800 ms (flash at time 0). The measuring frequency is 5000 Hz from −10 to 100 ms, 100 Hz otherwise. Preillumination treatment: 3 periods of 30 s illumination (Δt = 2 min). The total experiment was made with 8 different samples. (A) No wavelength selection (no interference filter), average of 1900 flashes. The different noise levels are due to the different measuring frequencies used during signal rise and decay. The scale was arbitrarily set to 1 for the signal at 60 ms (obtained from a linear fit between 60 and 100 ms). (B) Kinetics at 3 different wavelengths: 460 nm (black), 500 nm (red), 540 nm (blue). Averages of 2100 flashes at each wavelength. (C) Spectrum of 20 μM NADPH which was added to a cell suspension at 2.5 μg chl./ml (black; see Fig. S2). Spectrum obtained from kinetics similar to those of part B (green). The amplitudes were measured from the values at 60 ms (obtained from linear fits between 60 and 100 ms). Both spectra were normalized to 100 at 480 nm. Kinetics without interference filter were regularly intercalated between kinetics with interference filters, thus checking that the signal size remained constant during the whole experiment. For each signal, the baseline between −6 ms and 0 (flash time) was arbitrarily set to zero after fitting with a constant. The errors for the green spectrum are the sums of the errors resulting from fitting the baselines with constants and final signal levels with linear functions.

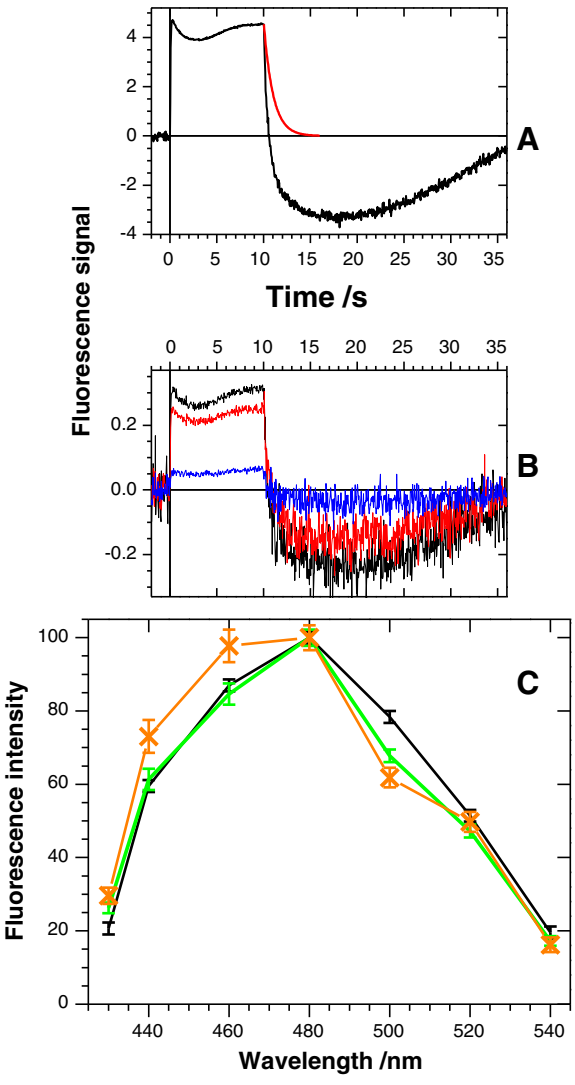

Fig. 2. Fluorescence kinetics induced by a 10 s illumination period. Actinic light intensity of 216 μmol m^{-2} s^{-1}. One measurement every 45 s. Cell suspension at a concentration of 2.5 μg chl./ml. The measuring frequency is 5000 Hz during illumination, 100 Hz otherwise. Preillumination treatment: 5 periods of 10 s illumination (Δt = 45 s). The total experiment was made with 10 different samples. (A) No interference filter, average of 585 measurements. The red line starting at 10 s is drawn arbitrarily for an illustrative purpose and corresponds to a monotonous exponential decay back to the baseline level. (B) Kinetics at 3 different wavelengths: 460 nm (black), 500 nm (red), 540 nm (blue). Averages of 240 measurements at each wavelength. (C) Spectrum of 20 μM NADPH (black; same spectrum as in Fig. 1); the green and orange spectra were obtained from kinetics similar to those of part B with the same interference filters as those of Fig. 1. The 3 spectra were normalized to 100 at 480 nm. The green spectrum corresponds to the maximum signal between 8 and 10 s after onset of illumination. The orange spectrum corresponds, with an inverted sign, to the minimum signal between 16 and 21 s. For the green and orange spectra, the amplitudes were determined by fitting with constants and the errors were calculated as for Fig. 1. Kinetics without interference filter were regularly intercalated between kinetics with interference filters, thus checking that the signal size remained constant during the measurements.

changes in ionic strength (50 mM NaCl and/or 5 mM $MgCl_2$) do not modify NADPH fluorescence at pH 8.

2.3. Chlorophyll a and photosystem I concentrations

The chl. *a* concentration was measured after methanol extraction using the absorption coefficient given in [15]. This was used to estimate the approximate PSI concentration. For this purpose, knowledge of the PSI/PSII ratio is a prerequisite. In a recent work on *Synechocystis* [16], a value of 5 for the PSI/PSII ratio was determined by biochemical methods. In this last study as well as in the present case, the cultures were grown at moderate light intensity (*c.* 50 μmol photons m^{-2} s^{-1}) with light exciting PBS more than chl. Under such conditions generally referred to as PSII light, ratio values of 2.5 to 10 were also found in other cyanobacterial strains [17]. We failed to determine precisely the PSI/PSII ratio by EPR [18] from the cultures used in this study due to the small intensity of the tyrosine-D radical signal (unpublished observations and personal communication from Dr. A. Boussac). These EPR experiments were consistent with a ratio larger than 4. Assuming conservatively a PSI/PSII ratio between 3 and 10 and taking into account

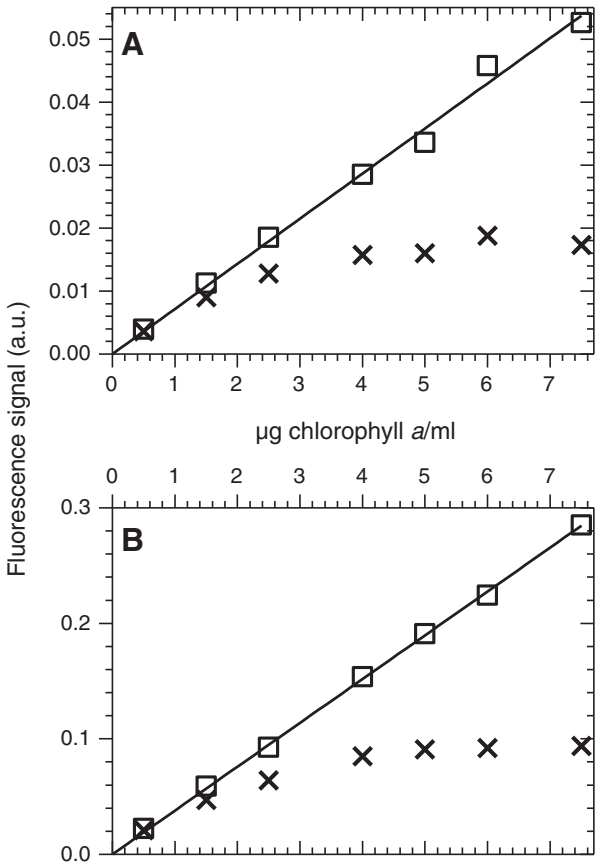

Fig. 3. Amplitude of NADPH fluorescence at different cell amounts. Measurements similar to those shown in Figs. 1A and 2A were performed at different chl. concentrations, from 0.5 to 7.5 µg chl./ml. Signal sizes exhibit a nonlinear saturation-like behavior when plotted as a function of chl. concentration, both for the signal elicited by a 10 µs flash (A) and the signal elicited by a 10 s illumination period (B). At each chl. concentration, 800 and 270 measurements were averaged for flash and continuous light experiments, respectively. After correction for the apparent transmission of the cell suspension (corrected signal = uncorrected signal/apparent transmission with apparent transmission = $10^{(-0.0644 \times \text{chl. in µg/ml})}$, see Fig. S4), the signals exhibit a linear dependence upon the chl. concentration (open squares). The lines in both parts result from linear regression fits.

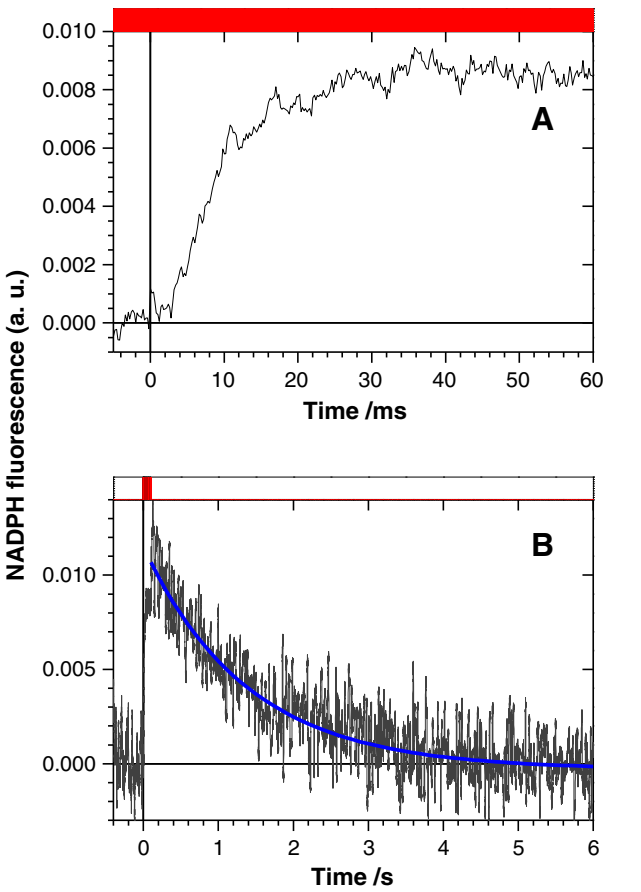

Fig. 4. Kinetics of NADPH formation and decay induced by a short flash (10 µs duration). One flash every 10 s. Average of 800 measurements. Cell suspension corresponding to 2.2 µg chl./ml. Preillumination treatment: 3 periods of 30 s illumination (Δt = 2 min). The red rectangles correspond to a high measuring frequency (5000 Hz). (A) The rising kinetics are shown after baseline subtraction (see Fig. S6). (B) The decay kinetics are shown without correction, thus explaining the larger initial amplitude of the signal than for the rising signal in (A). The decay is fitted with a single exponential phase of 0.96 s halftime (blue curve).

the number of chlorophylls per core photosystem (96 in PSI and 35 in PSII), the *in vivo* chl. to PSI ratio is expected to lie between 100 and 108. An intermediate value of 105 was used throughout the present study to calculate the *in vivo* PSI concentration from the chl. concentration.

2.4. Oxygen-evolution measurements

These measurements were made with the set-up described in [19]. Oxygen-evolving under saturating light (between 600 and 730 nm) as well as oxygen consumption in darkness were measured in parallel with NADPH measurements on a cell suspension at 5.5 µg chl./ml. During the initial dark period, O_2 consumption was *c.* 30 µmol mg^{-1} chl. h^{-1} and light excitation led to O_2 evolution at a rate of 193 µmol O_2 mg^{-1} chl. h^{-1}. This was followed by partial deoxygenation with argon flushing thus leading to a decreased dark O_2 consumption of 12 µmol mg^{-1} chl. h^{-1}. An evolution rate of 258 µmol O_2 mg^{-1} chl. h^{-1} was then measured under light.

3. Results

The light-induced signals that we will describe below are relatively small compared to the background fluorescence [9]. This impedes the evaluation of an absolute level of NADPH fluorescence and all measurements will be displayed with the dark signal preceding illumination arbitrarily set to zero. As we will describe light-induced changes, the fluorescence signals will be considered to arise from NADPH, which is initially produced by FNR during illumination. However it must be kept in mind that NADH and NADPH cannot be distinguished by fluorescence, so that NADH contributions to the signals cannot be excluded.

3.1. Kinetics and spectra after short flashes or during/after continuous light

Our first goal was to measure the spectrum of the fluorescence signal, in order to check that it arises from NADPH. Such experiments are shown with either short flashes of 10 µs duration (Fig. 1) or a 10 s continuous illumination (Fig. 2, same arbitrary units for both figures). The kinetics in part A of the figures were recorded with the colored broad-band filter (see the Material and methods section) whereas those in part B were measured at individual wavelengths by inserting interference filters between the colored filter and the PM. Spectra were thus obtained between 430 and 540 nm (part C) and were found to be similar to the fluorescence spectrum that was measured with the DUAL-PAM for exogenous NADPH added to a cell suspension at the same concentration (Fig. S1). This last spectrum exhibits a maximum at 480 nm, contrary to its known emission maximum peaking around 460 nm [20]. This distortion arises most probably from the properties of the interference filters used with the PAM (precise bandwidths and maximum transmissions are not identical). The present spectral

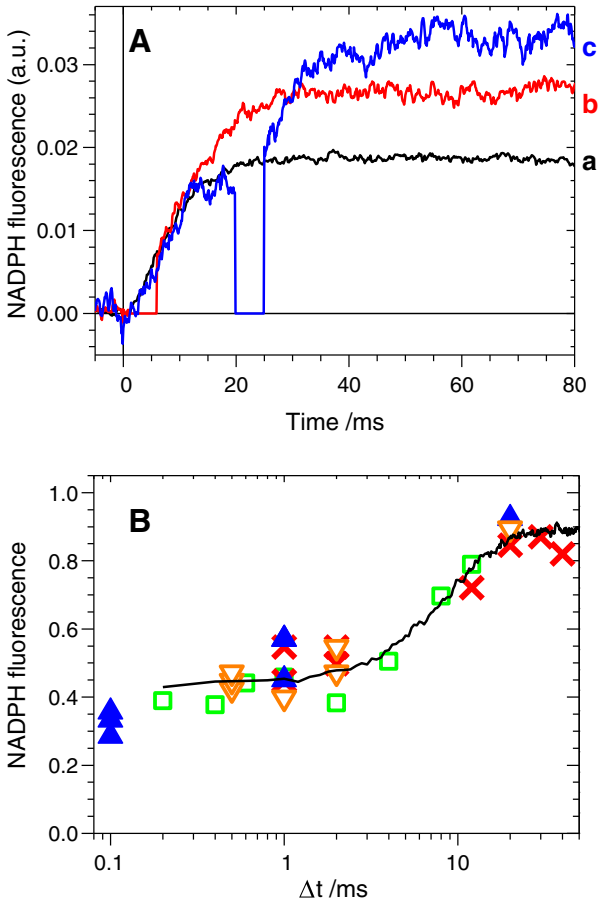

Fig. 5. Kinetics of NADPH formation in double flash experiments. (A) NADPH rising kinetics are compared for experiments involving a single laser flash (trace a, average of 2000 measurements), a laser flash followed by a 10 μs flash with time intervals between the two flashes of either 1 ms (trace b, average of 800 measurements) or 20 ms (trace c, average of 300 measurements). The same baseline (no flash) was subtracted from the three signals. The signal from the PM could not be measured for 5 ms after the 10 μs flash because part of the LEDs exciting light was facing the PM in the geometrical configuration used for these measurements (see the Material and methods section). It was checked that, in this configuration, there is no signal distortion 5 ms after the 10 μs flash. (B) The ratio of the second flash increment to the first flash amplitude is plotted as a function of the time interval between the two flashes, in logarithmic horizontal scale. The increment was measured at 40–60 ms after the 10 μs flash from differences such as (c–a) or (b–a) of part A. The different symbols correspond to measurements recorded during 4 different days, using similar samples as those studied in (A). Each symbol corresponds to an average of 200 to 800 measurements. The kinetics induced by a single laser flash are also shown after manual adjustment (vertical shift and multiplication for level adjustments at both 0.5–2 ms and 20–40 ms). Cell suspensions corresponding to 2.35 μg chl./ml; one measurement every 5 s; preillumination treatment for each sample: 3 periods of 45 s illumination (Δt = 2 min). For (B), the data were obtained from 8 different samples.

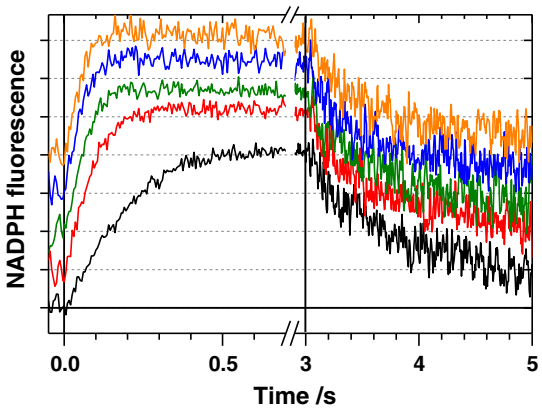

Fig. 6. NADPH kinetics induced by continuous light of different intensities. The fluorescence signals were recorded during and after illumination periods of 3 s at 5 different actinic light intensities (60, 126, 216, 531, 1287 μmol photons m^{-2} s^{-1} from bottom to top; The kinetics are shifted vertically for better visualization). One measurement every 20 s, average of 60 measurements for each light intensity.

results show that, in both types of measurements, the fluorescence signals arise mostly from NADPH (see the Discussion section). Besides this, different features of these kinetics can be noticed:

- After a 10 μs flash, the signal rise is almost completed at 30 ms and half of the signal rise has occurred in less than 10 ms. The signal then decays much more slowly.
- After the onset of continuous illumination, the initial fast rise is followed by a decay/rise feature leading to a plateau attained at about 8 s under these experimental conditions. Such complex kinetics have been already observed both for cyanobacteria [9,21] and the green alga *Chlorella vulgaris* [9], but have not been clearly interpreted yet (see the Discussion section).
- After the end of continuous illumination, a large undershoot is observed (the after-light level is transiently below the dark level), also in line with previous measurements [9,21]. Its spectrum (in orange in Fig. 2C) shows that it can be attributed to NADPH (and possibly partially to NADH). Processes of NADPH consumption have been therefore activated during the illumination period. Should this not be the case, the fluorescence signal would decay monotonously to the dark level (as illustrated by the drawn red curve in Fig. 2A).
- Comparing the amplitudes between Figs. 1 and 2 reveals that the NADPH amount formed during continuous illumination is about 4.5-fold the single flash amount, whereas the difference between the maximum level (at 8–10 s) and the minimum level (at 16–21 s) corresponds to 8 times the single flash signal. This suggests that the NADP pool is not very large compared to the PSI concentration.

A technical point is also worth mentioning: The noise levels appear to be different along with time. This is related to the measuring frequency, which needs to be adjusted in order to minimize the actinic effects of the measuring light [9] (see figures legends and the Material and methods section for further details).

3.2. The NADPH signals can be quantitatively estimated

The same signals as those measured in Figs. 1A and 2A were measured at different cell amounts. This is shown in Fig. 3A and B (crosses) as a function of chlorophyll (chl.) concentration. Both the signals elicited by a 10 μs flash and a 10 s light period deviate from linearity, even at the smallest concentrations that were studied, and reach a plateau at about 4 μg chl./ml. At concentrations above 10 μg/ml, the signals decrease with concentration (not shown). These observations can be attributed mostly to fluorescence reabsorption. Exogenous NADPH can be added to a cell suspension and its fluorescence can be measured in darkness (Figs. S1, S2 and S3). Its fluorescence signal remains constant for several minutes which shows that NADPH is not consumed or degraded during this time. For a given concentration of exogenous NADPH, the signal decreases with the cell concentration (Fig. S3) following an apparent Beer's law where the signal attenuation, when converted to apparent absorbance, increases linearly with chl. concentration (Fig. S4). When the *in vivo* light-induced signals are corrected for this apparent absorbance, a linear dependence is recovered between the signal intensities and the chl. concentration (open squares in Fig. 3A/B). These data show that measuring the exogenous NADPH fluorescence allows quantitative estimation of light-induced NADPH in cell suspensions at any chl. concentration up to 7.5 μg/ml. In most of our measurements, such a dark calibration was performed by adding, at the end of the experiment, a known amount of exogenous NADPH. Accordingly,

the amplitudes of the light-induced signals could in principle be given in units of NADPH concentrations. This quantification procedure will be applied and critically evaluated in the Discussion section.

3.3. Photosystem I photochemistry is saturated by 10 μs flashes

As 10 μs flashes provided with the DUAL-PAM were used extensively, we asked the question whether these flashes are saturating. Moreover, besides saturation, some double PSI turnover may occur within 10 μs, although this seems rather unlikely in view of our current knowledge of *in vivo* electron donation to $P700^+$ in *Synechocystis* (see *e.g.* [22]). Both issues (saturation and absence of double turnover) could be tested together by using an intense and short laser actinic flash which was synchronized with the DUAL-PAM acquisition. The same signal kinetics and amplitudes were observed for the 10 μs flash and the oversaturating laser pulse (Fig. S5). Identity of the two signals show that 10 μs flashes are most probably saturating and elicit single PSI turnover, as nanosecond laser flashes do.

3.4. Kinetics of NADPH formed after a single flash

The kinetics of NADPH formation and decay are shown in detail in Fig. 4. It was necessary to subtract a baseline contribution in order to measure the true rising kinetics (see Fig. S6, which corresponds to the same data set). After an initial lag lasting for 2–3 ms, the signal rises rapidly and reaches its full size in less than 40 ms, with half of the signal being formed in *c.* 8 ms (Fig. 4A). The signal decay after the flash (Fig. 4B) can be fitted with a single exponential component of $t_{1/2} =$ 0.96 s. The relatively large noise level during the decay is due to the low measuring frequency of the measuring light (see the Material and methods section). The "initial" (at 100 ms after the flash) size of the decaying signal is also larger than that seen in Fig. 4A. This is due to the fact that the raw signal is displayed in Fig. 4B after 100 ms, *i.e.* without subtracting the baseline updrift which is present during the first 100 ms after the flash.

3.5. Kinetics of NADPH formed after two consecutive flashes

We devised a double-flash experiment with different time intervals (hereafter named Δt) between the two flashes (6 ns laser flash followed by a 10 μs flash). The goal of this experiment was two-fold: Firstly, to compare the signal amplitude elicited by the second flash when Δt is just sufficient for the first-flash rise to be completed (Δt ≈ 20–40 ms) to the first flash amplitude. As this Δt is sufficient for $P700^+$ formed by the first flash to be completely reduced, the signal increment due to the second flash is expected to be of similar size to that of the first flash, provided that the environments (and therefore the fluorescence yields) of NADPH produced by the 2 flashes are identical. Secondly, to study the kinetics of NADPH formation for Δt as short as possible but long enough to elicit a second turnover in most of PSI. In such conditions of double PSI turnover, we may expect that this leads to an increase in the initial rate of NADPH formation by comparison to single-flash kinetics.

In Fig. 5A, double-flash experiments with Δt of 1 ms and 20 ms are compared to single laser-flash experiments. Three observations can be made from these comparisons: Firstly, the signals for both double-flash experiments are larger than for single flash (final levels of b and c above that of a). This was expectable as double PSI turnover should give more NADPH than single PSI turnover. Secondly, the signals for the two double-flash experiments are different with a significantly larger signal for the largest Δt (c above b at 40–80 ms). This may appear surprising at first sight as, in both cases, these are two PSI turnovers so that the amount of photoreduced acceptors should be the same. Thirdly, the initial rate in the double-flash experiment with Δt = 1 ms (b) is similar to that of the single flash experiment (a), and the two curves deviate only after *c.* 8–10 ms, as better seen in Fig. S7. This shows that increasing the amount of reduced ferredoxin or reduced PSI terminal acceptors above the single flash level does not lead to a higher initial rate of NADPH formation, thus pointing to a kinetic limitation.

The ratio of the second flash increment to the first flash amplitude is plotted in Fig. 5B as a function of Δt. Several features of this plot are noteworthy:

- A hardly visible increase for Δt between 0.1 and 0.5 ms: This is attributed to an increasing contribution of double PSI turnover in this time interval, as a significant part of P700 is still oxidized at 0.1 ms after the first flash and is reduced between 0.1 and 0.5 ms [23], so that the amount of reduced acceptors (ferredoxin and PSI terminal acceptors) resulting from PSI photochemistry increase with Δt.
- An almost constant level for Δt between 0.5 and 2 ms: This is attributed to a large and almost constant amount of double PSI turnover in this time interval. We performed preliminary *in vivo* flash-induced absorption kinetics in the near infra-red region (800/870 nm, data not shown) with a 30 μs time resolution. While these data support the fact that plastocyanin oxidation contributes to the infrared absorption changes, they also show that at most 20% of P700 is still oxidized at 0.5 ms after the flash, so that there is little $P700^+$ reduction between 0.5 and 2 ms after the 1st flash.
- A 2-fold increase for Δt between 2 and 40 ms, which cannot be attributed to an increase in the amount of double PSI turnover, as this last increase should be small in this time range (see above). The NADPH signal increase is attributed to the fact that, when the two flashes are relatively close in time, the resulting reductants cannot be used for NADPH formation as efficiently as when the flashes are well time-separated. This is also in agreement with a kinetic limitation of NADPH formation.
- The "asymptotic value" of the signal increment (Δt = 20–40 ms) corresponds to *c.* 90% of the 1st flash signal. This shows that the yield of NADPH fluorescence is about the same for the first and second flashes.

3.6. Rising kinetics and final amplitudes are not light-limited during continuous illumination

NADPH accumulation kinetics are shown in Fig. 6 for 5 different actinic-light intensities. The initial rate of NADPH formation increases at the smallest intensities and becomes constant at larger intensities. The final signal size under light is about the same at all light intensities. A small decrease in signal size is also observable at the highest intensities, an effect for which we have no explanation. The after-light decay is similar at all light intensities and is initially about 10-times slower than the signal rise at the largest light intensities. This indicates that the maximum level under light does not result from a competition between NADPH formation and decay.

3.7. NADPH consumption is activated by prolonged illumination

We studied the kinetics of dark NADPH decay following different times of illumination from 0.5 to 32 s. This is shown in Fig. 7, where increasing times of illumination alternate with dark periods of 2 min. Whereas the final level under light is similar in all cases, the size of the after-light signal undershoot increases with the illumination duration (as also shown in Fig. S8). This effect is largely reversed with the light duration of 0.5 s which ends the sequence. The initial dark decay kinetics depend also strongly on the illumination duration, as illustrated in Fig. 8, where the same data are plotted after adjusting the final light signals to the same fluorescence level. As initial rates of dark NADPH decay are difficult to measure due to a poor signal to noise ratio, this decay was quantified as the time necessary for dark consumption of an arbitrary NADPH amount, which can be visualized by a horizontal line in Fig. 8A. When the illumination time increases, this time decreases almost ten times from 1.3 s to 0.15 s and reaches a plateau above 16 s of

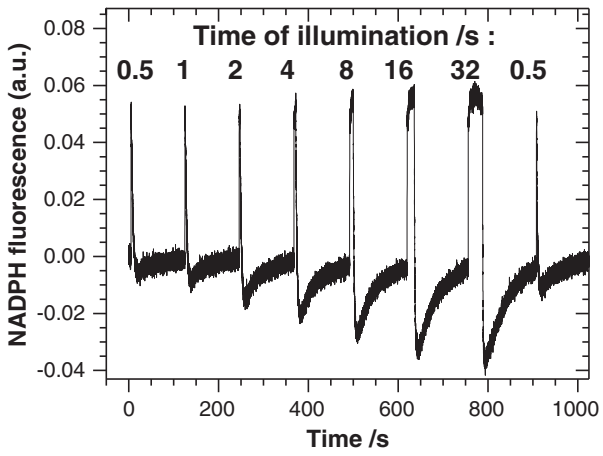

Fig. 7. After-light NADPH consumption depends upon the duration of the light period. The NADPH signal was measured during a sequence of illuminations of increasing duration (from 0.5 to 32 s; actinic light intensity of 340 μmol photons m^{-2} s^{-1}) with 2 min of darkness between consecutive light periods. The measurement ended with illumination for 0.5 s. Cell suspensions corresponding to 5.4 μg chl./ml; preillumination treatment: 3 periods of 30 s illumination ($\Delta t = 2$ min) followed by a dark period of 5 min.

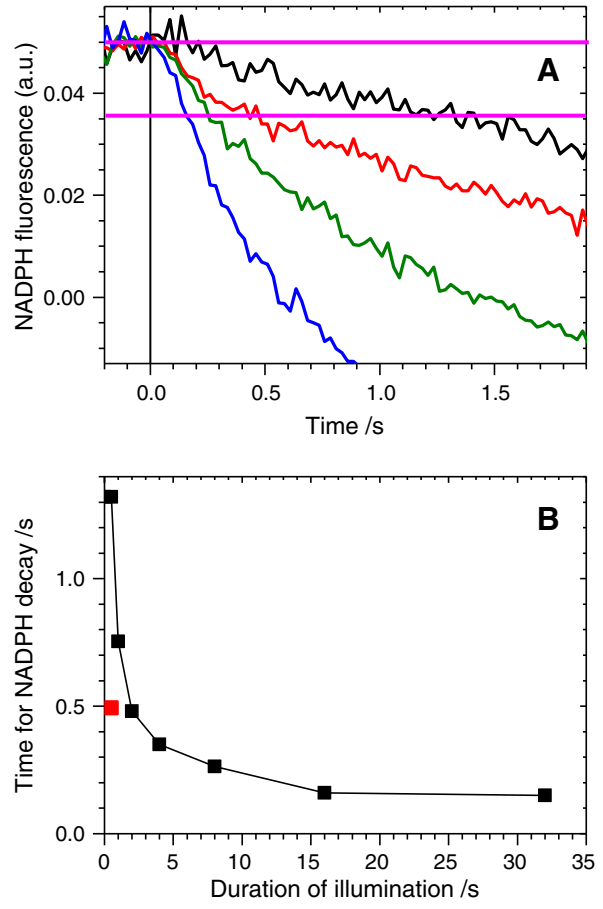

Fig. 8. The initial dark NADPH decay depends upon the duration of illumination. (A) shows the same data as in Fig. 7 for light durations of 0.5, 2, 8 and 32 s (upper to lower traces). The signals just before switching off the light were all set to the same fluorescence level (= upper horizontal line) for the purpose of comparison. Time zero corresponds to the end of illumination. (B) The initial dark NADPH consumptions were estimated from the time necessary for the signals to reach the lower horizontal line level in (A). The red square corresponds to the last 0.5 s light period. The difference between the two horizontal lines equals one apparent NADPH per PSI (see the Discussion section).

illumination (Fig. 8B). Reversal of the effect (measured from the last illumination duration of 0.5 s) appears to be partial in this case (red square in Fig. 8B). Both observables (initial dark decay and size of undershoot) can be explained by the activation of an NADPH-consuming process during light, which could well be the Calvin–Benson cycle. It can be also noticed that for illumination periods up to 3 min, kinetic characteristics (initial decay rate and size of undershoot) similar to those after 32 s were observed (data not shown). This indicates that there this no further visible change in NADPH consumption after 30 s of illumination.

4. Discussion

4.1. In vivo fluorescence spectra

In vivo fluorescence spectra measured either after a flash or during/after continuous illumination are similar to the spectrum of NADPH that was added to a cell suspension, hereafter named *in vitro* spectrum (Figs. 1C and 2C). However small but significant differences were observed between them. Whereas the two light-induced spectra are quite similar (green spectra in Figs. 1C and 2C), they both differ from the *in vitro* spectrum at 500 nm (black spectrum). A similar lack of signal at *c.* 500 nm is also observed for the after-light fluorescence undershoot (orange spectrum in Fig. 2C). We have no explanation for these observations. One may think of fluorescence quenching by a chromophore (carotenoid?) with an absorption maximum around 500 nm. The after-light undershoot spectrum also differs from other spectra by relatively larger signals below 480 nm. This suggests that NAD(P)H could be in different environments with varying contributions of the different NAD(P) subpopulations during continuous light measurements. Studying further the spectral characteristics of the fluorescence light-induced signals under different conditions and at different time scales might be certainly useful to further understand NAD(P)H formation and consumption.

4.2. NADPH is formed rapidly both after a flash and during continuous illumination

As already mentioned, it is quite possible that NADH contributes to part of the signals described in the present work. However, the fast signal rise following either a flash or the onset of high-intensity continuous illumination, is highly likely due to NADPH, which is produced by FNR from PSI-photoreduced ferredoxin. Similarly, the abrupt decay at the end of illumination is likely due to NADPH consumption by the activated Calvin–Benson cycle. After a single saturating flash (either laser flash of nanosecond duration or 10 μs flash provided with the DUAL-PAM), NADPH formation is almost completed within 40 ms with half of the signal rise observed at 8 ms after the flash. To our knowledge, this is the first report of *in vivo* flash-induced kinetics whereas similar kinetics have been previously observed only with intact spinach chloroplasts, albeit at a significantly slower rate ([9]; half signal rise at *c.* 30 ms). The kinetics observed in our work appear to be fast in view of the multiple successive steps which are involved in FNR catalysis [1]. This mechanism involves two successive reduction steps of the FAD cofactor of FNR by two reduced ferredoxins and hydride transfer from $FADH^-$ to $NADP^+$ [24,25]. Several protein–protein dissociation steps are also involved (reduced ferredoxin from PSI, oxidized ferredoxin from semi-reduced FNR). The lag of *c.* 2 ms which precedes signal rise is thus easily understandable as NADPH formation is the last event of a long sequence.

Under our growth conditions (photoautotrophy, exponential phase), the most part of FNR is present in its large PBS-bound isoform [3]. When observing the relatively fast kinetics of NADPH formation after a flash, this must be kept in mind together with the fact that two different reduced ferredoxins, being reduced by two different PSI complexes, are involved in a catalytic cycle. Supramolecular organization of the

thylakoid complexes/membrane(s) and PBS should accommodate the observed kinetics. Modifications in this supramolecular organization by mutations or growth conditions will be useful to understand how stringent this organization is for maintaining a high rate of NADPH formation.

4.3. Light-induced slow fluorescence changes

During continuous illumination, slowly varying fluorescence changes are occurring after the initial fast rise (Fig. 2A), as already observed [9]. Changes in NADH concentrations may contribute to such slowly varying signals. Other hypotheses dealing with changes in NADPH fluorescence will be discussed below. Electrochromic pigment absorbance shifts due to changes in membrane potential have been observed in plants and algae with kinetics under light similar to these slow changes (see *e.g.* [26,27]). This may suggest that the membrane potential could modify the NADPH fluorescence, by a yet unknown process. However testing this hypothesis requires to measure such electrochromic shifts in cyanobacteria, which, to our knowledge, have not been described yet. A local change of pH close to the cytoplasmic side of the membrane is also not expected to give any contribution, as NADPH fluorescence is constant in the pH range 7–10 (see the Material and methods section). It was also earlier proposed that the slow NADPH transients could be correlated to changes in chlorophyll fluorescence [9], thereby linking NADPH levels to changes in the PQ pool redox state. We tested this possibility by performing chlorophyll fluorescence measurements simultaneously with NADPH measurements with the DUAL-PAM. Moreover we measured with another PAM spectrometer $P700^+$ kinetics under similar conditions of light excitation. Both types of measurements (data not shown) could not be easily correlated to the NADPH fluorescence kinetics. Further work is therefore needed before any correlation between NADPH fluorescence and other *in vivo* probes can be possibly established.

4.4. In vivo enhancement of NADPH fluorescence

Measuring the fluorescence signal of exogenous NADPH added to a cell suspension allows, in principle, the vertical scale to be converted from arbitrary units to absolute NADPH concentrations (see Table 1 for absolute vertical scaling of data). For testing the validity of quantification, measurements with saturating laser and 10 μs flashes are appropriate because these flashes elicit single charge separation in all PSI reaction centers: As an example, the rising end-signal of Fig. 4A was found to correspond to an NADPH light-induced concentration of 22.5 nM, whereas the PSI concentration was 23.4 nM (as estimated with 5% uncertainty from the chl. concentration in the cell suspension; see the Material and methods section). As NADPH requires two electrons, provided by PSI-photoreduced ferredoxin, to be formed from $NADP^+$, a maximum NADPH concentration of 23.4/2 = 11.7 nM is expected (assuming that all electrons from PSI are involved in producing NADPH). In all experiments that we performed during this study with different cultures and different conditions of measurements (*e.g.* number, duration, periodicity of illumination periods before the flash measurements), the $NADPH_{single\ flash}$/PSI ratio was found to be comprised between 0.70 and 0.98, numbers which should be compared with a maximum expected value of 0.5. This shows that *in vivo* light-induced fluorescence is enhanced compared to fluorescence of exogenous NADPH.

The most simple explanation for these observations is that the fluorescence enhancement is due to FNR binding, as the yield of NAD(P)H fluorescence has been reported to increase with protein binding [12,20]. This possibility was tested by double-flash experiments (Fig. 5) eliciting double PSI turnover:

$$1\text{st flash} + \text{FNR} + NADP_1^+ \rightarrow \text{FNR-}NADPH_1$$

$$2\text{nd flash} + \text{FNR-}NADPH_1 + NADP_2^+ \rightarrow \text{FNR-}NADPH_2 + NADPH_1$$

where $NADP(H)_1$ and $NADP(H)_2$ are two different NADP(H) molecules. The above scheme assumes that FNR does not bind NADPH in darkness and, for the sake of simplicity, that each enzyme undergoes a single catalytic cycle after each flash.

Several other experimentally-based assumptions are implicit in this scheme: Firstly, NADPH has a much stronger affinity for FNR than $NADP^+$ with a K_d for NADPH of *c.* 0.8 μM being 6% that for $NADP^+$ [28]. Secondly, the *in vivo* FNR concentration, which lies in the 100 μM range [16], is much less than that of PSI (a PSI to FNR ratio of *c.* 4 was measured recently in *Synechocystis* [16]). It is therefore very likely that most of FNR will bind NADPH after completion of the first flash signal rise.

From the scheme, it appears that the second flash should give rise to an incremental production of NADPH which is not FNR-bound. However Fig. 5 shows that fluorescence enhancement occurs as well for the second flash increment (Fig. 5A: [PSI] ≈ 25 nM, the 1st flash signal and the 2nd flash increment with Δt = 20 ms correspond to NADPH apparent concentrations of *c.* 20 and 18 nM, respectively; see Table 1). From this, one can conclude that the fluorescence enhancement cannot be attributed solely to FNR binding. This means either that the *in vivo* fluorescence of free NADPH is also enhanced, or that $NADPH_1$ binds to another fluorescence-enhancing protein as soon as it is released from FNR. This last possibility is in line with [12] where it was concluded that most of NADPH is protein-bound in the chloroplasts. One can also note that, as the NADP pool is partially reduced in darkness under our experimental conditions (see below), FNR may bind NADPH in darkness. If this is the case, even the first flash fluorescence enhancement cannot be due to FNR binding.

4.5. $NADP^+$ photoreduction is kinetically limited and in competition with other processes: evidence for an FNR bottleneck

Two different features of the double-flash experiment point to a kinetic limitation of $NADP^+$ photoreduction: Firstly, whereas the expected amount of reduced ferredoxin or PSI terminal acceptors (hereafter named $(\text{Fd-PSI acc.})_{red}$) in double-flash measurements with Δt = 0.5–2 ms is almost twice larger than in single-flash

Table 1
Signal amplitudes and apparent NADPH concentrations. The last two columns allow the scale in figures to be converted into absolute NADPH concentrations and were calculated after addition of exogenous NADPH (2 to 4 μM) at the end of the light-induced measurements. The PSI concentration was calculated from the chl. *a* concentration by assuming an *in vivo* chl. to PSI ratio of 105.

Figure	PSI concentration (nM)	Signal corresponding to 1 apparent NADPH per PSI (a.u.)	Light-induced apparent NADPH concentration (nM)
Fig. 2A	26.6	1.06	115 (end of initial rise)
Fig. 4	23.4	0.00905	22.5 (40–60 ms)
Fig. 5A	25.0	0.0238	20 (laser; 40–60 ms)
Fig. 6	21.3	Scale unit × 0.85	94 (green curve)
Fig. 7	57.6	0.0143	190–230 (end of illuminations)

measurements, the initial rates of NADPH formation are similar (as shown for $\Delta t = 1$ ms in Fig. 5A). Secondly, in double-flash kinetics, the increment of NADPH due to the second flash increases two-fold when Δt varies from 2 to 40 ms, for an almost constant amount of $(\text{Fd-PSI acc.})_{red}$ (Fig. 5B). This last observation provides evidence that, when Δt is smaller than *c.* 10 ms, processes different from $NADP^+$ reduction efficiently consume $(\text{Fd-PSI acc.})_{red}$. These processes can be recombination reactions, cyclic electron transfer, superoxide formation and reduction of Fd partners other than FNR.

The yield of NADPH formation, *i.e.* the percentage of $(\text{Fd-PSI acc.})_{red}$ used for $NADP^+$ reduction, will be noted as ρ_{NADPH}. The aforementioned two-fold increase (when Δt varies from 2 to 40 ms) shows that ρ_{NADPH} is less than 0.5 for $(\text{Fd-PSI acc.})_{red}$ produced by the second-flash when Δt is in the range 0.5–2 ms (it will be *c.* 0.5 if the first flash ρ_{NADPH} is one; more generally, one has: $\rho_{NADPH,\ 2nd\ flash,\ \Delta t\ =\ 0.5\ -\ 2\ ms} \approx 0.5 \times \rho_{NADPH,\ 1st\ flash}$). In other words, our data show that more than 50% of $(\text{Fd-PSI acc.})_{red}$ can be used for processes other than $NADP^+$ reduction under a temporary overaccumulation of $(\text{Fd-PSI acc.})_{red}$ associated to fast double PSI turnover. The relatively small value of $\rho_{NADPH,\ 2nd\ flash,\ \Delta t\ =\ 0.5\ -\ 2\ ms}$ is consistent with a kinetic limitation in $NADP^+$ reduction.

Therefore the two above features can be attributed to a kinetic limitation which we call the FNR bottleneck. Such a denomination is supported by the observation that the size of the second-flash signal increment follows a Δt dependence (shown in Fig. 5B) which is superimposable to the kinetics of single flash NADPH formation (black curve of Fig. 5B): One can think that when NADPH is formed after the first flash by hydride transfer from $FADH^-$ to $NADP^+$, oxidized FAD becomes available for reduction by ferredoxin, thus relieving the FNR bottleneck, at the expense of other processes competing for $(\text{Fd-PSI acc.})_{red}$.

4.6. Estimation of the NADPH fluorescence enhancement in vivo

In vivo NADPH fluorescence is enhanced compared to that of exogenously added NADPH. The enhancement factor (hereafter called FEF, the fluorescence enhancement factor) is larger than 2 as the amount of the NADPH apparent concentration formed after a single flash can be as large as twice its expected maximum (Table 1 and Section 4.4). Besides a lower limit, we may try to determine an upper limit for the FEF: It is highly likely that the FEF is $\lesssim 4$ as a value larger than 4 gives less than one NADPH photoproduced per PSI (Table 1), which appears to be highly unlikely.

4.7. The light-dependent NADP pool: size and redox state

Data from Fig. 6 provide evidence that the maximum amount of NADPH is not limited by light or by a kinetic competition with the dark decay, which is much slower than the signal rise induced by high-intensity light. This indicates that the NADP pool is almost fully reduced under illumination of sufficient intensity. On the other hand, if one assumes that NADPH (*vs* NADH) consumption makes the major contribution to signal decay just after cessation of illumination, in line with the activation of the Calvin–Benson cycle, the lowest level of NADPH is observable after completion of the undershoot signal following continuous illumination (Figs. 2 and 7). As this decay is considerably faster than the subsequent dark NADPH formation (Figs. 7 and S8A), which may be attributed to the oxidative pentose phosphate pathway, the lowest level (at maximum extent of undershoot) should correspond to an almost fully oxidized NADP pool. From what precedes, the difference between the maximum and the minimum fluorescence levels observed under appropriate conditions (sufficient light intensity for observing the maximum signal and illumination of long enough duration for observing the minimum signal after undershoot) gives the approximate size of the light-dependent NADP pool. Using this method, we consistently found pool sizes comprised between 5.5 and 8 NADP per PSI, not taking into account the FEF. With an FEF of 2 to 4, this drops to NADP/PSI ratios between 1.4 and 4. Assuming 105 chlorophylls per PSI *in vivo* (see the Material and methods section), this corresponds to 15–43 nmol NADP/mg chl.

Assuming that most of the signal arises from NADPH and that its fluorescence yield is constant, our data indicate that the NADP pool is 30 to 50% reduced in darkness (see baseline levels in Figs. 2 and 7). This is similar to what was found in spinach chloroplasts ([29], pool 55% reduced). More recently, measurements of the pool redox state were performed in *Synechocystis*, without explicitly mentioning the dark/light conditions, and gave highly contrasting results (60% reduced in [30]; 75% reduced in [31]; entirely oxidized in [32]). It can also be noticed that no after-light undershoot was observed by Schreiber and Klughammer [9] with *c.* 2 min illumination of cyanobacterial suspensions, both in *Synechocystis* and in *Synechococcus* sp. PCC7942, whereas a large undershoot was observed by the same authors after a short and intense illumination following 5 min preillumination [9]. These differences may be due to differences in growth conditions or in cell history during the period between centrifugation/resuspension and signal acquisition. These factors may influence the energy state of the cells, thus affecting the different pathways consuming or producing NAD(P)H in darkness as well as modifying the conditions for activating the Calvin–Benson cycle.

4.8. The maximum rate of NADPH consumption after light is significantly smaller than the photosynthetic rate

Data of Fig. 6 were used to determine the time required for photoreduction of one apparent (disregarding the FEF) NADPH per PSI as a function of the actinic light intensity. This time decays from 105 ms to about 18 ms at intensities above 300 μmol photons $m^{-2}\ s^{-1}$ (Fig. S9). Similarly, data in Fig. 8A were used to estimate the initial NADPH consumption after prolonged illumination (the difference in horizontal magenta lines corresponds to one apparent NADPH per PSI): It takes 150 ms for decay of one apparent NADPH per PSI (Fig. 8B). A similar time (150 ± 20 ms) was determined for all samples studied with [PSI] between 20 and 30 nM and illumination periods between 16 and 180 s. Therefore there is an 8-fold ratio between the rates of maximum NADPH formation and consumption. Taking into account an FEF of 2–4 and PSI being quantified by assuming 105 chl. per PSI, the times of 18 and 150 ms determined above can be easily converted to more currently used units, *i.e.* 530–1070 and 64–128 μmol NADPH mg^{-1} chl. h^{-1} (NADPH photoproduction and initial dark consumption, respectively).

In parallel with NADPH measurements, we performed measurements of net oxygen evolution and found values of 193–258 μmol O_2 mg^{-1} chl. h^{-1}, in accordance with published values comprised between 150 and 400 μmol O_2 mg^{-1} chl. h^{-1} [33–36]. Assuming that NADPH is consumed entirely for CO_2 assimilation by the Calvin–Benson cycle with negligible photorespiration, the observed NADPH initial decay corresponds to a photosynthesis rate of 32–64 μmol CO_2 mg^{-1} chl. h^{-1}. This rate converts to a slightly higher of rate of oxygen evolution as, during linear electron transfer, part of the net electron flux may be used for other processes, *i.e.* essentially nitrogen assimilation. Nevertheless, our measurements of NADPH consumption appear to be at odds with the observed rate of oxygen evolution. Further work is needed to understand this discrepancy.

4.9. NADPH fluorescence as a versatile probe

Although fluorescence is not *a priori* a highly reliable technique when it comes to quantitation, we have shown here that the light-induced formation and subsequent decay of NADPH, as recorded by *in vivo* fluorescence, can provide semi-quantitative results for studying the energetic metabolism of cyanobacteria. The *in vivo* NADPH fluorescence was found to be enhanced, and the enhancement factor was estimated within a factor of 2. Our study paves the way for measuring the

NADPH *in vivo* kinetics and showed that flash kinetics can be used to further understand FNR catalysis *in vivo*. Many energetic processes can be studied with this technique, *e.g.* the activation and desactivation step(s) of the Calvin–Benson cycle, the relative electron fluxes involved in this last process and in competing ones (*e.g.* NADPH consumption by flavodiiron proteins [37], hydrogenase, nitrogen assimilation, *etc.*) and the cyclic and respiratory electron flows. As a general conclusion, the present study shows that NADPH fluorescence is an efficient probe for studying the energetic metabolism of cyanobacteria which can be used for assessing multiple phenomena occurring over different time scales.

Acknowledgements

We thank Dr. Ghada Ajlani for her continuous interest in this work, her help in growing cultures, stimulating discussions and critical reading of this article. We thank Dr. Diana Kirilovsky and Dr. Anja Krieger-Liszkay for critical reading of this article and stimulating discussions. We thank Dr. Alain Boussac for his help in measuring oxygen evolution. We were supported by a CEA/DSV "Bioénergie" Grant. P.S. was supported by the Agence Nationale de Recherche ANR-09-BLAN-0005-01.

Appendix A. Supplementary data

Supplementary data to this article can be found online at http://dx.doi.org/10.1016/j.bbabio.2014.01.009.

References

[1] N. Carrillo, E.A. Ceccarelli, Open questions in ferredoxin–$NADP^+$ reductase catalytic mechanism, Eur. J. Biochem. 270 (2003) 1900–1915.
[2] I. Lans, M. Medina, E. Rosta, G. Hummer, M. Garcia-Viloca, J.M. Lluch, A. Gonzalez-Lafont, Theoretical study of the mechanism of the hydride transfer between ferredoxin–$NADP^+$ reductase and $NADP^+$: the role of Tyr303, J. Am. Chem. Soc. 134 (2012) 20544–20553.
[3] J.C. Thomas, B. Ughy, B. Lagoutte, G. Ajlani, A second isoform of the ferredoxin:NADP oxidoreductase generated by an in-frame initiation of translation, Proc. Natl. Acad. Sci. U. S. A. 103 (2006) 18368–18373.
[4] A. Moolna, C.G. Bowsher, The physiological importance of photosynthetic ferredoxin $NADP^+$ oxidoreductase (FNR) isoforms in wheat, J. Exp. Bot. 61 (2010) 2669–2681.
[5] C. Gomez-Lojero, B. Perez-Gomez, G.Z. Shen, W.M. Schluchter, D.A. Bryant, Interaction of ferredoxin:$NADP^+$ oxidoreductase with phycobilisomes and phycobilisome substructures of the cyanobacterium *Synechococcus* sp strain PCC 7002, Biochemistry 42 (2003) 13800–13811.
[6] A.A. Arteni, G. Ajlani, E.J. Boekema, Structural organisation of phycobilisomes from *Synechocystis* sp strain PCC6803 and their interaction with the membrane, Biochim. Biophys. Acta 1787 (2009) 272–279.
[7] M. Twachtmann, B. Altmann, N. Muraki, I. Voss, S. Okutani, G. Kurisu, T. Hase, G.T. Hanke, N-terminal structure of maize ferredoxin:$NADP^+$ reductase determines recruitment into different thylakoid membrane complexes, Plant Cell 24 (2012) 2979–2991.
[8] W.M. Schluchter, D.A. Bryant, Molecular characterization of ferredoxin–$NADP^+$ oxidoreductase in cyanobacteria: cloning and sequence of the petH gene of *Synechococcus* sp. PCC 7002 and studies on the gene product, Biochemistry 31 (1992) 3092–3102.
[9] G. Schreiber, C. Klughammer, New NADPH/9-AA module for the DUAL-PAM-100: description, operation and examples of application, PAM Appl. Notes 2 (2009) 1–13.
[10] L.N.M. Duysens, J. Amesz, Fluorescence spectrophotometry of reduced phosphopyridine nucleotide in intact cells in the near-ultraviolet and visible region, Biochim. Biophys. Acta 24 (1957) 19–26.
[11] Z.G. Cerovic, E. Langrand, G. Latouche, F. Morales, I. Moya, Spectral characterization of NAD(P)H fluorescence in intact isolated chloroplasts and leaves: effect of chlorophyll concentration on reabsorption of blue-green fluorescence, Photosynth. Res. 56 (1998) 291–301.
[12] G. Latouche, Z.G. Cerovic, F. Montagnini, I. Moya, Light-induced changes of NADPH fluorescence in isolated chloroplasts: a spectral and fluorescence lifetime study, Biochim. Biophys. Acta 1460 (2000) 311–329.
[13] B. Ughy, G. Ajlani, Phycobilisome rod mutants in *Synechocystis* sp. strain PCC6803, Microbiol. 150 (2004) 4147–4156.
[14] B.L. Horecker, A. Kornberg, The extinction coefficients of the reduced band of pyridine nucleotides, J. Biol. Chem. 175 (1948) 385–390.
[15] R.J. Porra, W.A. Thompson, P.E. Kriedemann, Determination of accurate extinction coefficients and simultaneous equations for assaying chlorophylls *a* and *b* extracted with four different solvents: verification of the concentration of chlorophyll standards by atomic absorption spectroscopy, Biochim. Biophys. Acta 975 (1989) 384–394.
[16] G. Moal, B. Lagoutte, Photo-induced electron transfer from photosystem I to $NADP^+$: characterization and tentative simulation of the *in vivo* environment, Biochim. Biophys. Acta 1817 (2012) 1635–1645.
[17] Y. Fujita, A. Murakami, K. Aizawa, K. Ohki, Short-term and long-term adaptation of the photosynthetic apparatus: homeostatic properties of thylakoids, in: D.A. Bryant (Ed.), The Molecular Biology of Cyanobacteria, vol. 1, Kluwer Academic Publishers, Dordrecht, 1994, pp. 677–692.
[18] R. Danielsson, P.A. Albertsson, F. Mamedov, S. Styring, Quantification of photosystem I and II in different parts of the thylakoid membrane from spinach, Biochim. Biophys. Acta 1608 (2004) 53–61.
[19] N. Ishida, M. Sugiura, F. Rappaport, T.L. Lai, A.W. Rutherford, A. Boussac, Biosynthetic exchange of bromide for chloride and strontium for calcium in the photosystem II oxygen-evolving enzymes, J. Biol. Chem. 283 (2008) 13330–13340.
[20] T.G. Scott, R.D. Spencer, N.J. Leonard, G. Weber, Emission properties of NADH. Studies of fluorescence lifetimes and quantum efficiencies of NADH, AcpyADH, and simplified synthetic models, J. Am. Chem. Soc. 92 (1970) 687–695.
[21] H.L. Mi, C. Klughammer, U. Schreiber, Light-induced dynamic changes of NADPH fluorescence in *Synechocystis* PCC 6803 and its ndhB-defective mutant M55, Plant Cell Physiol. 41 (2000) 1129–1135.
[22] R.V. Duran, M. Hervas, M.A. De la Rosa, J.A. Navarro, The efficient functioning of photosynthesis and respiration in *Synechocystis* sp PCC 6803 strictly requires the presence of either cytochrome c_6 or plastocyanin, J. Biol. Chem. 279 (2004) 7229–7233.
[23] R.V. Duran, S. Hervas, M.A. De la Rosa, J.A. Navarro, In vivo photosystem I reduction in thermophilic and mesophilic cyanobacteria: the thermal resistance of the process is limited by factors other than the unfolding of the partners, Biochem. Biophys. Res. Commun. 334 (2005) 170–175.
[24] C.J. Batie, H. Kamin, Electron transfer by ferredoxin:$NADP^+$ reductase. Rapid-reaction evidence for participation of a ternary complex, J. Biol. Chem. 259 (1984) 11976–11985.
[25] C.J. Batie, H. Kamin, Ferredoxin:$NADP^+$ oxidoreductase. Equilibria in binary and ternary complexes with $NADP^+$ and ferredoxin, J. Biol. Chem. 259 (1984) 8832–8839.
[26] D.M. Kramer, C.A. Sacksteder, A diffused-optics flash kinetic spectrophotometer (DOFS) for measurements of absorbance changes in intact plants in the steady-state, Photosynth. Res. 56 (1998) 103–112.
[27] B. Bailleul, P. Cardol, C. Breyton, G. Finazzi, Electrochromism: a useful probe to study algal photosynthesis, Photosynth. Res. 106 (2010) 179–189.
[28] C.J. Batie, H. Kamin, Association of ferredoxin–$NADP^+$ reductase with NADP(H) specificity and oxidation–reduction properties, J. Biol. Chem. 261 (1986) 11214–11223.
[29] U. Takahama, M. Shimizu-Takahama, U. Heber, The redox state of the NADP system in illuminated chloroplasts, Biochim. Biophys. Acta 637 (1981) 530–539.
[30] H. Takahashi, H. Uchimiya, Y. Hihara, Difference in metabolite levels between photoautotrophic and photomixotrophic cultures of *Synechocystis* sp. PCC 6803 examined by capillary electrophoresis electrospray ionization mass spectrometry, J. Exp. Bot. 59 (2008) 3009–3018.
[31] J.W. Cooley, W.F.J. Vermaas, Succinate dehydrogenase and other respiratory pathways in thylakoid membranes of *Synechocystis* sp strain PCC 6803: capacity comparisons and physiological function, J. Bacteriol. 183 (2001) 4251–4258.
[32] T. Osanai, A. Oikawa, T. Shirai, A. Kuwahara, H. Iijima, K. Tanaka, M. Ikeuchi, A. Kondo, K. Saito, M.Y. Hirai, Capillary electrophoresis-mass spectrometry reveals the distribution of carbon metabolites during nitrogen starvation in *Synechocystis* sp. PCC 6803, Environ. Microbiol. 16 (2013) 512–524.
[33] J.J. Benschop, M.R. Badger, G.D. Price, Characterisation of CO_2 and HCO_3^- uptake in the cyanobacterium *Synechocystis* sp PCC6803, Photosynth. Res. 77 (2003) 117–126.
[34] W. Majeed, Y. Zhang, Y. Xue, S. Ranade, R.N. Blue, Q. Wang, Q.F. He, RpaA regulates the accumulation of monomeric photosystem I and PsbA under high light conditions in *Synechocystis* sp PCC 6803, PLoS One 7 (2012) e45139.
[35] T. Wallner, Y. Hagiwara, G. Bernat, R. Sobotka, E.J. Reijerse, N. Frankenberg-Dinkel, A. Wilde, Inactivation of the conserved open reading frame ycf34 of *Synechocystis* sp PCC 6803 interferes with the photosynthetic electron transport chain, Biochim. Biophys. Acta 1817 (2012) 2016–2026.
[36] Q.J. Wang, A. Singh, H. Li, L. Nedbal, L.A. Sherman, Govindjee, J. Whitmarsh, Net light-induced oxygen evolution in photosystem I deletion mutants of the cyanobacterium *Synechocystis* sp PCC 6803, Biochim. Biophys. Acta 1817 (2012) 792–801.
[37] Y. Allahverdiyeva, H. Mustila, M. Ermakova, L. Bersanini, P. Richaud, G. Ajlani, N. Battchikova, L. Cournac, E.M. Aro, Flavodiiron proteins Flv1 and Flv3 enable cyanobacterial growth and photosynthesis under fluctuating light, Proc. Natl. Acad. Sci. U. S. A. 110 (2013) 4111–4116.